

# Composite Iodine-gold Nanoparticles as a Contrast Agent in Computed Tomography

Rezvan Ravanfar Haghighi<sup>1</sup>, Fariba Zarei<sup>1,2</sup>, Samira Moshiri<sup>1</sup>, Anahita Jafari<sup>1</sup>, Sabyasachi Chatterjee<sup>3</sup>, Vyas Akondi<sup>4</sup>, Vani Vardhan Chatterjee<sup>5</sup>

<sup>1</sup>Medical Imaging Research Center, <sup>2</sup>Department of Radiology, Shiraz University of Medical Sciences, Shiraz, Iran, <sup>3</sup>Retired Scientist from Indian Institute of Astrophysics; Ongil, 79 D3, Sivaya Nagar Reddiyar, Alagapuram, Tamil Nadu, <sup>4</sup>Department of Physical Sciences, Indian Institute of Science Education and Research, Government ITI Building, Berhampur, Odisha, India, <sup>5</sup>Department of Applied Physics and Instrumentation, Indian Institute of Science, Bengaluru, Karnataka, India

## Abstract

**Purpose:** Solutions of iodine-based compounds, due to their high X-ray attenuation coefficient, are widely used as contrast agents in computed tomography (CT) imaging. This paper investigates the attenuation properties of iodine and gold to develop nanoparticle-based contrast agents, for example, composite nanoparticles (NPs) with layers of iodine and gold or a mixture of NPs of gold and iodine. **Materials and Methods:** A theoretical formula is derived that gives the Hounsfield Unit (HU) for different weight-by-weight (w/w) concentrations of a mixture of blood + iodine + gold. The range of compositions for which iodine + gold mixture can give a suitable HU  $\geq 250$  upon being mixed with blood, is formulated. These estimates are derived from experiments on the variation of HU values in different compositions of aqueous solutions of iodine and available data for gold. **Results:** It is seen that for an aqueous solution of iodine, the suitable HU of 250 (hence giving sufficient gray level to the CT image) can be obtained with w/w concentrations of iodine being 0.0044, 0.008, and 0.0097 for observations at 80, 100, and 120 kVp, respectively. The corresponding w/w concentrations of gold NPs would be 0.0103, 0.0131, and 0.0158. With these basic results, compositions of suitable mixtures of iodine and gold are also specified. **Conclusion:** Aqueous suspensions of gold NPs are suitable as contrast materials for CT imaging and can also be used as a component of a composite contrast material consisting of an iodine and gold mixture.

**Keywords:** Computed tomography, contrast agent, nanoparticles

Received on: 22-09-2023

Review completed on: 02-04-2024

Accepted on: 16-05-2024

Published on: 21-09-2024

## INTRODUCTION

Computed tomography (CT) is nowadays widely used for noninvasive medical diagnosis. It graphically shows the internal structures of the material on a computer screen. For medical diagnostics, this visual aid is used by the doctor, who uses different gray levels in the image to discriminate between various structures in the patient's body. This ability to visually distinguish is greatly enhanced by injecting a material with a high X-ray attenuation coefficient into the patient's body. This material, called a "contrast agent," generally contains iodine or barium compounds. On injection or being orally administered into the bloodstream and gastrointestinal system of the body, it produces high X-ray attenuation in the organs that it permeates, creating brighter gray scales in the visual image.<sup>[1,2]</sup>

This advantage of using iodine, however, does not bring "unmixed" benefits due to the fast washout and kidney toxicity

of iodine-bearing compounds. For the expulsion of iodine from the body, the contrast has to pass through the kidney and may cause damage in the course of its "excursion" and "residence" there. Mainly for this reason, substitutes for iodine are sought, and gold nanoparticles (AuNPs) are proposed by many researchers as suitable candidates because gold is chemically inert and considered to be nontoxic. However, the main interest in nanoparticles (NPs) arises because of their ability to navigate slowly through the body (long flush-out time) and collect in large numbers in certain affected cells.<sup>[3-5]</sup> In other words, the main aim of using NPs is to have particles

**Address for correspondence:** Dr. Rezvan Ravanfar Haghighi, Medical Imaging Research Center, 8<sup>th</sup> Floor, Research Tower, Khalili Street, Shiraz, Iran.  
E-mail: sravanfarr@gmail.com

### Access this article online

Quick Response Code:



Website:  
www.jmp.org.in

DOI:  
10.4103/jmp.jmp\_126\_23

This is an open access journal, and articles are distributed under the terms of the Creative Commons Attribution-NonCommercial-ShareAlike 4.0 License, which allows others to remix, tweak, and build upon the work non-commercially, as long as appropriate credit is given and the new creations are licensed under the identical terms.

**For reprints contact:** WKHLRPMedknow\_reprints@wolterskluwer.com

**How to cite this article:** Haghighi RR, Zarei F, Moshiri S, Jafari A, Chatterjee S, Akondi V, *et al.* Composite iodine-gold nanoparticles as a contrast agent in computed tomography. J Med Phys 2024;49:448-55.

whose mixing time with blood flow and flushing time from the body are long and which can adhere to specific organs of the body for a long time. Trials have been made by several groups with polyethylene glycol (PEG) covered AuNPs of diameters in the range of 28–30 nm. It has been found on trial with mice that these PEG-covered AuNPs can collect in large amounts in certain parts of the body, rendering them distinctly visible in CT images for about 48 h.<sup>[6,7]</sup>

One other reason for selecting gold is its high X-ray attenuation property. Although many have claimed gold to be a more suitable material for attenuation than iodine, we have, however, pointed out that for CT sources at  $V = 80, 100, 120$ , and  $140$  KVp, the effective mass attenuation coefficients lie in the range of  $22.1\text{--}7.57\text{ cm}^2/\text{g}$  for iodine and  $12.98\text{--}4.52\text{ cm}^2/\text{g}$  for gold.<sup>[8,9]</sup>

This means that for the same amount of substance, iodine can attenuate the energy flux more than one can achieve with gold. Detailed studies about the relative merits of iodine and AuNP have recently been published.<sup>[10]</sup> It is shown in the above publication that “iodine outperformed AuNPs in terms of contrast to noise ratio.”

It is for the above reason that the full potential of iodine as a contrast agent (CA) should be examined. Attempts should be made to fabricate viable NPs of iodine with functional groups that are compatible with blood and can attach to certain cells. We are encouraged to present this idea since iodine and PEG-covered AuNPs have been fabricated in the past.<sup>[11]</sup>

For some unknown reason, not much attention was given to exploring the potential of such composite NP systems for application as CA systems in CT imaging. We suggest composite NPs of the type of structure given in Figure 1a and b and examine their X-ray attenuation properties depending on the relative proportions of gold and iodine.

It is to be noted that the targeting ability of the given structure depends upon the properties of the outer layer. Hence, we have suggested the outer layer be made of PEG, which can bind with both gold and iodine. Of the two structures given in Figure 1a and b, the one in Figure 1b may be mechanically more stable

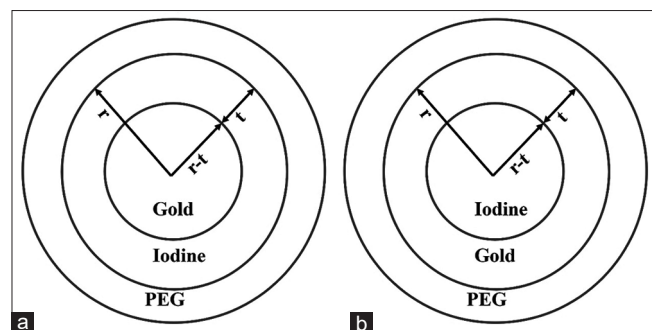


**Figure 1:** (a and b) Schematic diagram of a proposed composite nanoparticle. Two possible alternatives are given in cases. PEG: Polyethylene glycol

since layers of gold act as a protective cover for the brittle core of iodine. It is to be further noted that for any NP system, made of a single component or multicomponent materials, the X-ray attenuation per unit mass of the NP depends on the composition of the system and is independent of the NP's shape or size or on the relative arrangement of material substances.<sup>[9,12]</sup>

The paper is organized as follows: In the material and methods section, we first consider the X-ray attenuation properties of a mixture of iodine + gold + blood, as the HU values that are recorded are due to the above combination, the contributions from the outer PEG layers are negligible. Calculations are done for a uniform mixture of the above components for different compositions of the mixture since the total attenuation is independent of the shape, size, and arrangement of gold and iodine in the NPs. To know the effective attenuation coefficients of iodine and gold for X-ray source spectra available in the CT systems, we perform HU measurements of aqueous solutions of iodine at different concentrations. From this, the effective attenuation coefficient of iodine is first estimated, from which we next estimate the effective energy of the CT source spectrum using the national institute of standards and technology (NIST) tables. Finally, from this estimated value of the effective energy, we estimate the effective attenuation coefficient of gold for observations with CT systems at different kVps. These estimated numbers are used for the computation of HU values of blood + iodine + gold mixtures for different compositions. In this way, we derive a method by which the HU value of a given mixture can be approximated, and one can also ascertain the necessary composition of the mixture for any HU that may be required. This is particularly important since for fool-proof diagnostic imaging, HU values lying between 200 and 400 are recommended for diagnostic radiology.<sup>[13,14]</sup>

## MATERIALS AND METHODS

### Theory

We considered here a system composed of a mixture of blood, iodine, and gold. Since the density and mass attenuation coefficient of blood and water are similar, we considered that the mixture of blood and contrast was essentially a ternary mixture, containing water, iodine, and gold, for which we used the suffixes, “w,” “i,” and “g,” respectively.

Let  $w_w$ ,  $w_i$ , and  $w_g$  be the weight/weight concentrations of the three substances in the mixture, and let  $\rho_w$ ,  $\rho_i$ ,  $\rho_g$  be the respective densities of water, iodine, and gold, at room temperature. Given that the total mass of the mixture is  $M$ , the amounts of these quantities in terms of mass are,

$$M_w = M \times w_w; M_i = M \times w_i; M_g = M \times w_g \quad (\text{Eq. 1})$$

with

$$w_w + w_i + w_g = 1 \quad (\text{Eq. 2})$$

and their respective volumes are,

$$V_w = M_w/\rho_w; V_i = M_i/\rho_i; V_g = M_g/\rho_g \quad (\text{Eq. 3})$$

The total volume of the mixture is then,

$$V = V_w + V_i + V_g = M [(w_w/\rho_w) + (w_i/\rho_i) + (w_g/\rho_g)] \quad (\text{Eq. 4})$$

with the assumption that the volume of mixing is negligible. Thus, the mixture has a density,

$$\rho_{\text{mix}} = M/V = \rho_w \rho_i \rho_g / [\rho_w \rho_i w_g + \rho_g \rho_i w_w + \rho_w \rho_g w_i] \quad (\text{Eq. 5})$$

In practical situations, it is necessary to express the concentration in terms of the mass of the component per unit volume of the mixture. The concentrations are expressed as  $x_i, x_w, x_g$ , which are seen to be,

$$x_i = M_i/V = w_i / [(w_i/\rho_i) + (w_w/\rho_w) + (w_g/\rho_g)] = w_i / [(1/\rho_w) + w_i [(1/\rho_i) - (1/\rho_w)] + w_g [(1/\rho_g) - (1/\rho_w)]]$$

$$x_w = M_w/V = w_w / [(w_i/\rho_i) + (w_w/\rho_w) + (w_g/\rho_g)] = w_w / [(1/\rho_w) + w_i [(1/\rho_i) - (1/\rho_w)] + w_g [(1/\rho_g) - (1/\rho_w)]]$$

$$x_g = M_g/V = w_g / [(w_i/\rho_i) + (w_w/\rho_w) + (w_g/\rho_g)] = w_g / [(1/\rho_w) + w_i [(1/\rho_i) - (1/\rho_w)] + w_g [(1/\rho_g) - (1/\rho_w)]] \quad (\text{Eq. 6})$$

where we have used,  $w_w = 1 - w_i - w_g$  as given by Eq. 2 to obtain the extreme right-hand side expressions in Eq. 6. It can be seen that for low concentrations of iodine and gold, we have,  $w_i \ll 1$ ,  $w_g \ll 1$ , so the equations in Eq. 6 can be approximated as,  $x_w \approx w_w/\rho_w = 1000w_w$ ;  $x_i \approx w_i/\rho_i = 1000w_i$ ;  $x_g \approx w_g/\rho_g = 1000w_g$  (Eq. 7)

where we have substituted, the density of water to be  $\rho_w = 1000$  mg/mL, to express  $x_w, x_i, x_g$  in units of mg/mL of the substance.

Let  $X_w, X_i$ , and  $X_g$  be the mass attenuation coefficients of the substances at a given X-ray photon energy, being defined as the ratio: x-ray attenuation coefficient of the substance/its density. Then, the mass attenuation coefficient of the mixture is, known to be<sup>[15,16]</sup>

$$X_{\text{mix}} = X_w w_w + X_i w_i + X_g w_g \quad (\text{Eq. 8})$$

and its X-ray attenuation coefficient is given by,<sup>[15-17]</sup>

$$\mu_{\text{mix}} = \rho_{\text{mix}} X_{\text{mix}} \quad (\text{Eq. 9})$$

From the definition of the Hounsfield number (HU),<sup>[18]</sup>

$$HU = 1000 [\mu_{\text{mix}} - \mu_w] / \mu_w \quad (\text{Eq. 10})$$

it then follows that,

$$\mu_{\text{mix}} = \mu_w F \quad (\text{Eq. 11})$$

where we have defined,

$$F = 1 + (HU/1000) \quad (\text{Eq. 12})$$

Combining Eqs. 5-9, 11 and using  $w_w = 1 - w_i - w_g$ , as in Eq. 2, we get the relation

$$A w_g + B w_i + C = 0 \quad (\text{Eq. 13}),$$

where,

$$A = (\rho_w - \rho_g) \rho_i X_w F + \rho_g \rho_i (X_w - X_g) \quad (\text{Eq. 14})$$

$$B = (\rho_w - \rho_i) \rho_g X_w F + \rho_g \rho_i (X_w - X_i) \quad (\text{Eq. 15})$$

$$C = \rho_g \rho_i X_w [F - 1] \quad (\text{Eq. 16})$$

Eqs. 13-16 give a linear relation that describes the dependence of  $F$  and hence of the HU values on the w/w concentrations  $w_g$  and  $w_i$ , for any set of values with,  $0 \leq w_i, w_g < 1$ .

Further from the definition (Eq. 10) one has.

$$F = \mu_{\text{mix}} / \mu_w = X_{\text{mix}} \rho_{\text{mix}} / X_w \rho_w \quad (\text{Eq. 16})$$

so that on using (Eq. 7) for  $X_{\text{mix}}$ , (Eq. 5) for  $\rho_{\text{mix}}$  and  $w_w = 1 - w_i - w_g$ , as given in Eq. 2, we have,

$$F = N/D \quad (\text{Eq. 17})$$

where,

$$N = \rho_i \rho_g [X_w + (X_i - X_w) w_i + (X_g - X_w) w_g] \quad (\text{Eq. 18})$$

$$D = X_w [\rho_i (\rho_i - \rho_g) w_g + \rho_g (\rho_w - \rho_i) w_i + \rho_i \rho_g] \quad (\text{Eq. 19})$$

The corresponding HU values can be calculated using  $HU = 1000 (F - 1)$ , once the value of  $F$  is known.

Special cases: A. Water-iodine mixture,  $w_g = 0$ , so that we have,

$$F = \{ \rho_i [X_w + (X_i - X_w) w_i] / X_w [(\rho_w - \rho_i) w_i + \rho_i] \} \quad (\text{Eq. 20})$$

which for  $w_i \ll 1$ , can be approximated on expanding as a Binomial expansion,

$$1 / [(\rho_w - \rho_i) w_i + \rho_i] = (1/\rho_i) \times \{ 1 + [(\rho_w - \rho_i)/\rho_i] w_i \}^{-1} \approx (1/\rho_i) \times \{ 1 - [(\rho_w - \rho_i)/\rho_i] w_i \} \quad (\text{Eq. 21})$$

This gives (Eq. 20) as,

$$F - 1 = b_i w_i \quad (\text{Eq. 22})$$

where,

$$b_i = (X_i/X_w) - (\rho_w/\rho_i) \quad (\text{Eq. 23})$$

By using  $F - 1 = HU/1000$  and using Eq. 7 to convert  $w_i$  to  $x_i$  (using  $w_g = 0$ ), Eq. 21 also gives,

$$HU = b_i x_i \quad (\text{Eq. 24})$$

$x_i$  being expressed in units of mg/mL, as explained earlier.

B. For water-AuNP mixture,  $w_i = 0.0$ . By following the same steps as in case A, we have

$$F - 1 = b_g w_g \quad (\text{Eq. 25}),$$

with

$$b_g = (X_g/X_w) - (\rho_w/\rho_g) \quad (\text{Eq. 26}),$$

$$HU = b_g x_g \quad (\text{Eq. 27}),$$

$x_g$  being expressed in units of mg/mL.

Using the same approximation,  $0 \leq w_i, w_g \ll 1$ , we get from Eqs. 17-19 by using binomial expansions (Eq. 21),

$$HU = b_i x_i + b_g x_g \quad (\text{Eq. 28}).$$

## Experimental

To check the differences in gray level that human eyes can distinguish,<sup>[18]</sup> we filled a phantom with aqueous solutions having different concentrations of iodinated contrast. The phantom is

capable of holding 12 different samples simultaneously; its construction design and details are given.<sup>[19]</sup> The advantage of using this phantom is that images of substances with 12 different HU values can be shown in the same slice, and simultaneous visual comparison is possible. In this study, to evaluate the HU values quantitatively and visually, 8 different concentrations of contrast agents were used.

1, 2, 2.5, 3, 4, 4.5, 5, and 5.5 weight/weight percentages were prepared very accurately. A vial of OMNIPAQU 350 mg/mL, with the chemical formula  $C_{19}H_{26}N_3I_3O_9$ , was used as a stock to make the mentioned concentrations. The weights were measured by a balance with 0.001 g accuracy, and density measurement was done by the method of a specific gravity bottle.<sup>[20]</sup>

Test tubes containing different liquids were mounted in the 8 holes in the outer row of the phantom.

The inner test tubes were filled with 2, 3, and 4% contrast solutions to evaluate the beam hardening effect, which, however, is not central to this paper. The phantom, containing different concentrations of contrast solutions, was scanned at 80, 100, and 120 kVp with automatic tube current modulation (mAs was about 110), 0.7 s rotation time, pitch factor equal to 1, by a 16-multidetector GE LightSpeed CT system. Axial slices of 5 mm were reconstructed. Oval-shaped regions of interest, or ROI, were put inside the solution (without contamination with neighboring structures) to read the mean HU values. The mean HU values of all concentrations of contrast solutions, which were measured three times for each solution, were used to calibrate the CT system to determine effective energy at each peak voltage of 80, 100, and 120 kVp.

By this method, the value of the coefficient  $b_i$  in Eqs. 22, 24 was determined, which must correspond to  $b_i = \{(\langle X_i \rangle / \langle X_w \rangle) - (\rho_w / \rho_i)\}$  as given in Eq. 23, where  $\langle \dots \rangle$  denotes the average over the source spectrum of the CT machine. From the values for iodine given in the NIST tables, we determined the energy for which this observed value of  $b_i$  was obtained. We assigned this energy as the effective energy  $\langle E \rangle$  of the source spectrum. We next used the NIST table values for gold at energy  $\langle E \rangle$  for determining the corresponding value of  $b_g$ .

In different experimental works, AuNP suspensions were studied by different groups in which the gold NPs had a typical diameter of 10–100 nm.<sup>[6,21,22]</sup> The gold concentrations in the suspensions were typically between 0.0 and 10 mg/mL. The present paper, therefore, estimated the HU variations within this range of concentrations of gold and iodine.

## RESULTS

In Figure 2a and b, the CT images of aqueous solutions with different concentrations of iodinated contrast agents are shown. The mean ROI area that was used to measure the HU value of solutions was 30 mm<sup>2</sup>, containing (FOV = 250 mm, matrix size 512 × 512) about 120 pixels on average. As predicted, the HU values increased with increasing contrast agent concentration,

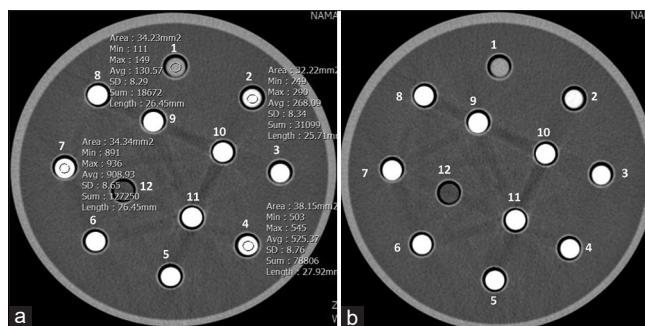


**Figure 2:** Axial slice of computed tomography images taken at 120 kVp with a window width of 450 and a window level of 45. In (a) Region of interest (ROI) and their related Hounsfield unit (HU) values for some test tubes (1, 2, 3.5, and 5 percentages of weight/weight concentration of contrast solution) are displayed, and, (b) Shows the images without the HU values for the w/w concentration of iodine to be  $w_i = 1, 2, 2.5, 3, 3.5, 4, 4.5, 5$ , and 5.5 in an outer row; the images for  $w_i = 2, 3, 4, 0.0$  are in the inner circle

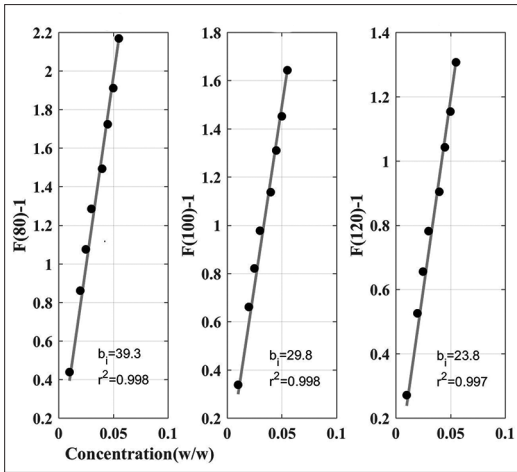
as can be seen in Figure 2a and b. The ROIs and related HU values for the 1<sup>st</sup>, 2<sup>nd</sup>, 4<sup>th</sup>, and 7<sup>th</sup> test tubes are shown. These contained 1%, 2%, 3%, and 5% weight/weight concentration solutions of iodinated contrast agents, respectively [Figure 2a]. The shade of gray in test tube number 1 with  $HU_{mean} = 130$  can be visually distinguished from that of others, whose HU values lie in the range of 250–1000. The gray scales of these images were observed in the mediastinal window with window width = 450 and window level = 45. High HU values cannot be discriminated against, as can be seen in Figure 2b.

Figure 3 shows the variation of [F-1] versus the w/w iodine concentration. It can be seen that the [F-1] versus  $w_i$  relation is approximately linear for iodine solution in water as given in Eq. 22, in the concentration range under study. By making the least squares fit between [F-1] versus  $w_i$  as given by Eq. 22, we found that  $b_i = 39.3, 29.8$ , and 23.8 for  $V = 80, 100$ , and 120 kVp, respectively.

In Table 1, the NIST table was used to find the values of  $X_w$ ,  $X_p$ , and  $X_g$  at different energies to determine the corresponding values of  $[X_i/X_w]$ ,  $[X_g/X_w]$ . These numbers,  $[X_i/X_w]$  and  $[X_g/X_w]$  are also displayed in Figure 4. From the values of  $b_i$  as given in Figure 3, the corresponding values of  $[X_i/X_w]$  for iodine were found. By referring to Figure 4, [or linear interpolation of the numbers given in Table 1], the corresponding energies at which these values of  $[X_i/X_w]$  occur were found. It can be concluded as a good approximation that these energies corresponded to the effective energies of the source spectrum, which were found to be  $\langle E \rangle = 58, 66, 73$  keV for the X-ray tube being excited at  $V = 80, 100, 120$  kVp. Then the values of  $[X_g/X_w]_{E=\langle E \rangle}$  at these energies  $\langle E \rangle$  in the three cases were found by linear interpolation from the values given in Table 1, which should also correspond to the graphical estimates from Figure 4. From the definition,  $b_g = [X_g/X_w] - (\rho_w/\rho_g)$ , the corresponding  $b_g$  values were concluded as,  $b_g = [X_g/X_w]_{E=\langle E \rangle} - (\rho_w/\rho_g)$ . These estimated values of  $b_g$  are displayed in Table 2.

With these estimates of  $b_i$  and  $b_g$ , given in Table 2, the predicted variation of HU versus  $w_i$ ,  $w_g$ , is plotted in Figure 5, using





**Figure 3:** The least-square fit of (a)  $[F(80)-1]$ , (b)  $[F(100)-1]$  and, (c)  $[F(120)-1]$  versus different concentrations ( $w_i$ ) of iodine contrast solutions in weight/weight ( $w/w$ ). The coefficients  $b_i = [(X_i/X_w) - (\rho_w/\rho_i)]$  in Eq. 17 are 39.3, 29.8, and 23.8 at 80, 100, and 120 kVp. The  $P$  values in all three cases are  $P < 0.001$

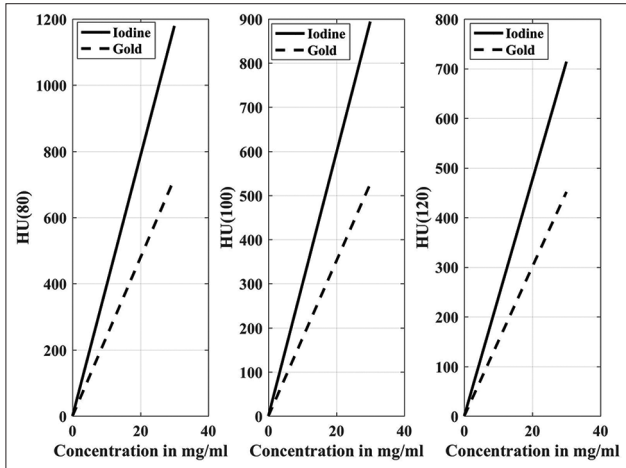


**Figure 5:** Predicted variations of Hounsfield unit versus concentration in mg/mL for iodine (solid curve) and gold (broken curve). The X-axis refers to  $x_i$  and  $x_g$  for iodine and gold, respectively. HU: Hounsfield unit

Eqs. 24, 27. The predicted curves for gold have a smaller slope than that of iodine, indicating that a higher HU value can be obtained for iodine than for gold when the same  $w/w$  concentrations were used.

Figure 6 depicts the  $(w_i, w_g)$  relationship that satisfies the HU value of the composite to be 250. This graph was generated using Eq. 28 and the values of  $b_i, b_g$  that were given in [Table 2]. It is seen that the line is tilted toward the y-axis since  $b_g < b_i$  i.e., for a single component system one needs a greater concentration of gold in mg/mL (iodine absent) than iodine in mg/mL concentration (gold absent).

### Estimates for a gold-capped iodine nanoparticle

Let us consider a gold-capped iodine nanoparticle of the type shown in Figure 1b. The total radius of the NP is " $r$ ," in which there is an outer layer of gold that has a thickness " $t$ ."

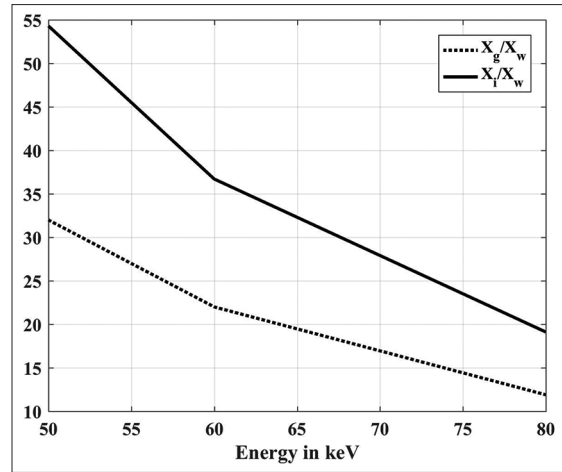


**Figure 4:** This figure depicts  $[X(E)/X_w(E)]$  for iodine and gold at  $E = 50, 60, 80$  keV. The estimated  $[X_g(E)/X_w(E)]$  values for 100, 120 kVp are found to lie far below the value at  $E = 80.72$  keV-the K-edge energy of gold, hence the values above 80 keV are ignored for the purpose of interpolation

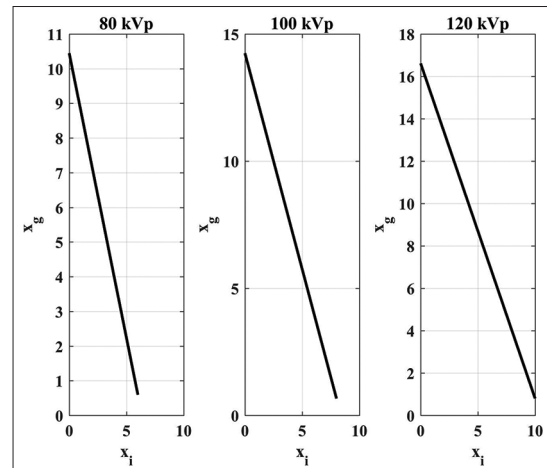


**Figure 6:** The relative concentration of iodine and gold ( $x_i, x_g$ ) for maintaining the Hounsfield unit of the mixture fixed at 250, for  $V = 80, 100, 120$  kVp

**Table 1: Record of mass attenuation coefficients  $X_{\text{gold}}$ ,  $X_{\text{iodine}}$ ,  $X_{\text{water}}$  for gold, iodine, and water at energies of interest, as given in the NIST tables**

E in keV	$X_{\text{gold}}$	$X_{\text{iodine}}$	$X_{\text{water}}$	$X_{\text{gold}}/X_{\text{water}}$	$X_{\text{iodine}}/X_{\text{water}}$
50	7.258	12.32	0.2269	31.99	54.3
60	4.529	7.557	0.2059	21.9961	36.7
80	2.185	3.51	0.1837	11.8944	19.11
80.07	8.902	3.51	0.1837	48.50	19.1

NIST: National institute of standards and technology

Then, the masses of iodine and gold in the composite NP are,  $m_i = (4 \pi/3) \rho_i (r-t)^3$  and  $m_g = 4 \pi \rho_g [r^3 - (r-t)^3]$ , respectively. We consider  $r = 20$  nm and  $t = 3$  nm. The value of  $t$  is decided by the observations by different groups that gold layers with thicknesses  $< 3$  nm are mechanically unstable.<sup>[23,24]</sup> Thus, with

**Table 2: Estimates of the effective energies  $\langle E \rangle$  and  $b_g$  for different kVp values**

V in keV	$b_i$ from Figure 3	$X_i/X_w = b_i + 0.2$	$\langle E \rangle$ in keV	$X_g/X_w$ at $\langle E \rangle$ , from NIST table	$b_g = (X_g/X_w) - 0.052$ from estimation
80	39.30	39.50	58	23.99	23.93
100	29.80	30.00	68	17.50	17.05
120	23.80	24.00	74	15.00	14.95

$X_g$ :  $X_{\text{gold}}$ ,  $X_i$ :  $X_{\text{iodine}}$ ,  $X_w$ :  $X_{\text{water}}$ , NIST: National institute of standards and technology

$\rho_i = 4.93 \text{ g/mL}$  and  $\rho_g = 19.3 \text{ g/mL}$ , we have  $m_i = 3.04 \times 10^{-16} \text{ g}$  and  $m_g = 7.94 \times 10^{-17} \text{ g}$ , i.e.,  $m_g/m_i = 0.25$ .

We now suppose that a certain quantity of this composite is to be added to the blood to have  $HU = 250$  at 80 kVp. The mixture of blood and NPs will have  $x_g = 0.25 x_i$  and  $HU = 250 = b_i x_i + b_g x_g = 39.50 x_i + 23.93 x_g = 39.50 x_i + 23.93 \times 0.25 x_i = 45.48 x_i$  giving  $x_i = 5.50 \text{ mg/mL}$  and  $x_g = 0.25 x_i = 1.37 \text{ mg/mL}$ .

This amount, when mixed with 5 L of blood (as in an adult male), requires 27.48 g of iodine, and 6.87 g of gold must be injected into the body through these NPs. However, if the contrast is to be provided by iodine NPs (i.e., without a gold cap), one must have  $x_i = 250/b_i = 6.33 \text{ mg/mL}$ , i.e., a total of 32 g of iodine to be mixed with 5 L of blood. In contrast, if the same  $HU = 250$  has to be obtained purely by adding gold alone (i.e., in the absence of iodine), the total amount of gold needed for 5 L of blood should be 52.25 g of gold. In similar steps, calculations can be done for iodine-gold NPs of various compositions and different HU values at different kVps. In doing these computations, it has to be kept in mind that the HU values are determined only by the composition of the mixture and not by the shape and size of the NPs or the relative arrangements of different layers.<sup>[9,12]</sup>

This possibility is only tentative. The above cases of gold multilayer formation are not dependent on iodine but on materials that are useful for electronic device fabrication. Such multilayer formations are strongly dependent on the surface properties of the surfaces and their mutual affinity. However, iodine and many organic compounds can be absorbed on the surface of gold (and many other transition metals). This has been effectively used to prepare a material of the type given in Figure 1a. The idea that we propose here is to use the same properties to make structures of the type given in Figure 1b, which we have discussed here.

### Estimates for iodine-capped gold cap

This corresponds to the case given in Figure 1a. The masses of gold iodine and are then  $m_g = (4 \pi/3) \rho_g (r-t)^3$  and  $m_i = 4 \pi \rho_i [r^3 - (r-t)^3]$ . Unfortunately, iodine binds to the surface of gold by chemisorption, i.e., forms only a single layer. As reported by March,<sup>[10]</sup> the addition of a surface layer of gold improves X-ray attenuation but such a material is bound to be costly since it is predominantly composed of gold, with iodine lying only on a single layer on the surface.

In both the cases A and B given in this section, we have ignored the contribution from the PEG whose attenuation is negligible and whose thickness is assumed to be small.

## DISCUSSION

The idea of developing viable, nontoxic CT contrast agents is a challenge for the scientific community. PEG-covered gold NPs are being specially investigated for this purpose because of their long flush-out time and also due to their capacity to bind for a long time and in large amounts to many structures within the body, thus giving high-contrast visibility to these parts. In presenting these possibilities with AuNP suspensions, it is claimed by many that AuNPs are better contrast agents than iodine because of gold's higher attenuation coefficient. This assertion has to be qualified, as we have pointed out in a recent publication.<sup>[9]</sup> In the above paper, we have estimated the mass attenuation coefficients of gold and iodine over the source spectrum of a typical X-ray source and have shown that this source-spectrum averaged mass attenuation coefficient of iodine is greater than that of gold for  $V = 80, 100$ , and  $120 \text{ kVp}$ , where in the last two cases, gold's high attenuation properties near its K-edge have been included. Most importantly, the estimates of 80 kVp given in the present paper match very well with the experimental findings with gold NPs, as reported by Dong *et al.*<sup>[6]</sup> For example, it is stated in the above paper that at 80 kVp ( $\Delta HU/\Delta x_i$ ), i.e., iodine is found to be 23.7 per mg/mL, whereas our estimated value is  $b_g = 23.93$  per mg/mL. The estimates for 100 and 120 kVp in the paper also lead to the same conclusion, as  $b_i > b_g$ , as given in Table 2. More accurate predictions can be drawn if the exact dependence of the source spectrum of the X-ray source and detector efficiency in the CT machine is known. In the absence of this information, we have made predictions based on energy estimates found with iodine data. The striking closeness of our estimated value of  $b_g$  with the values given by Dong *et al.*<sup>[6]</sup> suggests the reasonable of our method: although some leeway may be possible, the results are not expected to differ a great deal. We plan to check these estimates through direct experiments with  $\text{AuCl}_4$  solutions and AuNPs suspended in water. In examining the potential of PEG-gold-capped iodine NPs, we note that PEG is capable of binding with both gold and iodine, as shown by the successful fabrication of PEG-iodine-capped gold NPs.<sup>[11]</sup> This corresponds to the case shown in Figure 1a. Our suggestion is to remove gold altogether and use PEG-covered iodine NPs so that iodine provides attenuation and PEG gives binding to the cells. However, considering the brittleness of iodine, we have considered the case of PEG-gold-covered iodine NPs [Figure 1b] so that the gold cover gives mechanical stability to the system. For this, we have made estimates with the thickness of the gold cover being 3 nm. In this case, the amount of gold that has to be injected into the body of an

adult patient will still be high ~7–10 g. However, as gold binds to iodine through chemisorption, the thickness of the gold layer may be restricted to a single layer, and the costs may be economical.

Given the enormous costs of gold, any gold-based contrast will be impractical for mass-scale use, and we recommend that the full potential of iodine be exploited. A PEG-covered iodine NP can suit this purpose since PEG bonds with iodine,<sup>[11]</sup> and the outer layer of PEG is essential for the NPs' attachment to organs in the body. Alternatively, attempts should be made to replace gold with cheaper substances or bind iodine directly to PEG, which is possible as shown in.<sup>[11]</sup> Finally, the stability of such a system to surface rupture, etc., has to be investigated.<sup>[25]</sup> One is further encouraged by the results of March<sup>[10]</sup> which show that iodine "outperforms" gold in terms of contrast and also favorably vis-a-vis toxicity.

Two important issues need to be addressed. It has been observed that smaller-sized NPs are more effective in binding to the body's blood flow. However, smaller particles also mix more easily with any flowing liquid. Using the well-known Stoke's formula that the mixing time for a sphere of radius "*r*" is  $\tau_{mix} = 2\rho r^2/9\eta$  where  $\rho$  is the density of the sphere (19.3 g/mL for gold) and  $\eta$  is the viscosity of the liquid (0.055 P for blood), we find that for  $r = 10$  nm,  $\tau_{mix} = 10^{-10}$  s which is too small to explain the long mixing time (30 min) of AuNPs in blood. This mixing thus has to do more with biophysical mechanisms than mere molecular diffusion. Furthermore, the ability of composite NPs to attach to the walls of the organs has to be understood through detailed biophysical mechanisms. The same should be the approach to understanding the long time scales (~24 h) for AuNPs to remain attached to the walls of the organs. Both mechanisms, i.e., attachment and release, must be complex processes, and simple explanations through physics alone will not work.

Finally, it is to be noted that the formulae given in the paper apply to any system and the X-ray attenuation properties depend only on the chemical composition of the system.<sup>[9]</sup>

These formulae are thus valid for multiple-layered NPs or for multiple-layered NPs being suspended in liquids. These equations can thus be applied to contrast agents consisting of a suspension of multilayered NPs surrounded by common iodine-based contrasts. As far as the present paper is concerned, the major challenge is preparing NPs of the type given in Figure 1b. Although initial success has been reported for the preparation of NPs of type 1a,<sup>[11]</sup> for some unknown reasons, this kind of work has not been pursued by many other groups. The most important would be to eliminate gold and cover iodine NPs with suitable polymeric layers with mechanical stability and strength.

## CONCLUSION

In the search for viable CT contrast materials, as substitutes for iodine-based ones, PEG-covered gold NPs are now being

explored, due to these NPs' long flush-out time and high X-ray attenuation coefficient of gold. The present paper points out that in terms of attenuating ability per unit mass, iodine "outperforms" gold for CT imaging at 80, 10, 120, and 140 kVp, i.e. for the usual kVps that are available in commercial CT machines. This implies that for achieving the same level of attenuation; hence contrast, a lower amount of iodine is adequate than gold. This is an extremely important issue particularly due to gold's prohibitive costs. Complete abandonment of iodine being thus impractical; this paper considers the possibility of designing composite NPs, comprising gold and iodine, covered with PEG layers. Such composite NPs are to be used in preparing a liquid suspension that can be injected as a contrast material. The results of the present paper act as basic theoretical guides for designing and fabricating such viable CT contrast material, which can give necessary attenuation at affordable costs. This paper focuses on the X-ray attenuation properties of composites, which are to be used as guiding inputs, other inputs being related to the transportation of these NPs in the body and their adherence to the walls of different organs.

## Acknowledgment

The authors thank the Shiraz University of Medical Sciences for their encouragement and financial support of project number 23999.

## Financial support and sponsorship

This work was supported by Shiraz University of Medical Sciences (project number 23999), Shiraz, Iran.

## Conflicts of interest

There are no conflicts of interest.

## REFERENCES

1. Lusic H, Grinstaff MW. X-ray-computed tomography contrast agents. *Chem Rev* 2013;113:1641-66.
2. DeMaio DN. Mosby's Exam Review for Computed Tomography-E-Book. 2nd Edition: Elsevier Health Sciences; 2017.
3. Andreucci M, Solomon R, Tasanarong A. Side effects of radiographic contrast media: Pathogenesis, risk factors, and prevention. *Biomed Res Int* 2014;2014:741018.
4. Nagayama Y, Tanoue S, Tsuji A, Urata J, Furusawa M, Oda S, *et al.* Application of 80-kVp scan and raw data-based iterative reconstruction for reduced iodine load abdominal-pelvic CT in patients at risk of contrast-induced nephropathy referred for oncological assessment: Effects on radiation dose, image quality and renal function. *Br J Radiol* 2018;91:20170632.
5. Aschoff AJ, Catalano C, Kirchin MA, Krix M, Albrecht T. Low radiation dose in computed tomography: The role of iodine. *Br J Radiol* 2017;90:20170079.
6. Dong YC, Hajfathalian M, Maidment PS, Hsu JC, Naha PC, Si-Mohamed S, *et al.* Effect of gold nanoparticle size on their properties as contrast agents for computed tomography. *Sci Rep* 2019;9:14912.
7. Jiang Z, Zhang M, Li P, Wang Y, Fu Q. Nanomaterial-based CT contrast agents and their applications in image-guided therapy. *Theranostics* 2023;13:483-509.
8. Hubbell JH. Tables of X-ray Mass Attenuation Coefficients and Mass Energy-Absorption Coefficients; 1996.
9. Haghighi R, Chatterjee S, Zarei F, Jafari A, Vani VC, Pishdad P, *et al.* Effect of Aspect Ratio on the X-ray Attenuation of Nanoparticles: A Theoretical Study Radiation Physics and Chemistry; 2024. p. 111626.

10. March, L.M., *Hyperspectral X-ray Imaging: A Comparison of Iodinated and Gold Nanoparticle Contrast Media for the Application of Contrast-Enhanced Digital Mammography*; 2020.
11. Kim SH, Kim EM, Lee CM, Kim DW, Lim ST, Sohn MH, *et al.* Synthesis of PEG-iodine-capped gold nanoparticles and their contrast enhancement in *in vitro* and *in vivo* for X-ray/CT. *Journal of Nanomaterials* 2012;2012:46.
12. Haghighi RR, Chatterjee S, Chatterjee VV, Hosseinipناه S, Tadrissinik F. Dependence of the effective mass attenuation coefficient of gold nanoparticles on its radius. *Phys Med* 2022;95:25-31.
13. Damm R, Mohnike K, Gazis A, Rogits B, Seidensticker M, Rieke J, *et al.* Improvement of contrast media enhancement in CTA evaluating pulmonary embolism by utilizing 'delayed' bolus tracking in the descending aorta. *Pol J Radiol* 2016;81:422-7.
14. Oda S, Utsunomiya D, Nakaura T, Kidoh M, Funama Y, Tsujita K, *et al.* Basic concepts of contrast injection protocols for coronary computed tomography angiography. *Curr Cardiol Rev* 2019;15:24-9.
15. Khan F. *The Physics of Radiation Therapy*. 2<sup>nd</sup> ed. Baltimore, MD: Williams and Wilkins; 1994.
16. Johns HE, Cunningham JR. *The Physics of Radiology*. 4th Edition. pp:140-143. Charles C Thomas Publisher, Springfield, Illinois, USA; 1983.
17. Jackson DF, Hawkes DJ. X-ray attenuation coefficients of elements and mixtures. *Physics Reports* 1981;70:169-233.
18. Seeram E. *Computed Tomography Physical Principles, Clinical Application, and Quality Control*. 2<sup>nd</sup> ed. Philadelphia, Pennsylvania: W. B Saunders Company; 2001.
19. Haghighi RR, Chatterjee S, Sefidbakht S, Jalli R, Vani VC. Design and construction of an affordable phantom for electron density measurement and linearity tests of computed tomography systems. *Iran J Med Phys*. 2020;17:38-47.
20. Sartorius balance, Secura 1103-1s, made in Germany.
21. Mohajeri M, Iranpour P, Vahidi Y, Haghighi RR, Faghih Z, Bararjanian M, *et al.* Pegylated deoxycholic acid coated gold nanoparticles as a highly stable CT contrast agent. *Chemistry Select* 2020;5:9119-26.
22. Iranpour P, Ajamian M, Safavi A, Iranpoor N, Abbaspour A, Javanmardi S. Synthesis of highly stable and biocompatible gold nanoparticles for use as a new X-ray contrast agent. *J Mater Sci Mater Med* 2018;29:48.
23. Akolozina D, Kravets VG, Berdyugin AI, Grigorenko AN. Optical constants and optical anisotropy of ultrathin gold films. *Advanced Photonics Research* 2024;5:20300238.
24. Switzer JA, Hill JC, Mahenderkar NK, Liu YC. Nanometer-thick gold on silicon as a proxy for single-crystal gold for the electrodeposition of epitaxial cuprous oxide thin films. *ACS Appl Mater Interfaces* 2016;8:15828-37.
25. Chang J. *Capillary Wrinkling and Mechanical Properties: Single Layers, Bilayers, and Composites*; 2019.